Shahid Bahonar University of Kerman

Biomechanism and Bioenergy Research

Online ISSN: 2821-1855
Homepage: https://bbr.uk.ac.ir

Iranian Society of Agricultural Machinery Engineering and Mechanization

Introducing a Rapid and Practical Approach for Determining Fat Content in Cow Milk Using Image Processing

Lena Beheshti Moghadam[1], Seyed Saeid Mohtasebi[1]✉, Behzad Nouri[1], Mahmoud Omid[1], Seyed Morteza Mohtasebi[1]

[1] Department of Agricultural Machinery Engineering, Faculty of Agriculture, University of Tehran, Karaj, Iran.
✉ Corresponding author: mohtaseb@ut.ac.ir

ARTICLE INFO

Article type:

Research Article

Article history:

Received 06 July 2024

Received in revised form 23 October 2024

Accepted 24 October 2024

Available Online 31 December 2024

Keywords:

Non-destructive Analysis, Artificial neural network, Color, Milk, Quality Assessment, Fat Content, Cow Milk.

ABSTRACT

Milk fat content serves as a crucial indicator of milk quality, holding significance for both producers and consumers. Therefore, the development of a swift and viable method for assessing this parameter could greatly enhance monitoring efforts. This study aimed to establish a correlation between milk fat content and milk color through image analysis techniques. Cow milk samples spanning a fat content range of 0.2% to 3.5% were analyzed under various lighting conditions, employing a fusion of image processing methods with artificial neural networks (ANNs) and particle swarm optimization (PSO) algorithms. Results demonstrated that the most optimal method, determined through comparative analysis against a reference sample, produced accurate estimations of milk fat content. Statistical evaluation revealed a high coefficient of determination (R^2=0.99), accompanied by minimal mean absolute error (MAE=0.22) and mean squared error (MSE=0.05). Additionally, a comprehensive examination was conducted into the influence of water content on milk color across different levels of fat concentration. Findings from this investigation provided robust validation for the effectiveness of the proposed method, exhibiting attributes of reliability, efficiency, and cost-effectiveness in the realm of milk fat content assessment.

Cite this article: Beheshti Moghadam, L., Mohtasebi, S. S., Nouri, B., Omid, M., & Mohtasebi, S. M (2024). Introducing a Rapid and Practical Approach for Determining Fat Content in Cow Milk Using Image Processing. *Biomechanism and Bioenergy Research*, *3*(2), 61-74. https://doi.org/10.22103/bbr.2024.23712.1087

Publisher: Shahid Bahonar University of Kerman
DOI: https://doi.org/10.22103/bbr.2024.23712.1087

INTRODUCTION

Milk is a crucial dairy product within the human diet, owing to its abundant macronutrient composition. Ensuring its quality and content throughout the production journey, from farm to consumer, is imperative (Eid et al., 2022). Furthermore, fat constitutes a noteworthy component of the daily human diet due to its high energy density and appealing flavor profile (Mu et al., 2022). Moreover, milk fat plays a vital role in the average growth, brain development, visual acuity, and immunity of newborn ruminants. Its significance extends to disease prevention and treatment (Ali, 2022; Moate et al., 2018). Research by Pluschke et al. underscored undesirable metabolic effects, including diminished microbial protein synthesis, milk fat content, and fiber digestion (Pluschke et al., 2016).

Numerous endeavors have been made to measure milk fat content, aiming to establish tools for swift assessment of milk properties (Gallier et al., 2010). Milk with varying fat levels is characterized by its appearance, texture, and taste (Li et al., 2021; McCarthy et al., 2017; Soukoulis et al., 2010). Recent explorations into milk fat assessment have encompassed innovative technologies and methodologies, including fluorescent sensors (Xu et al., 2014), Spectral-sensitive Pulsed Photometry (Ragni et al., 2016), confocal Raman microscopy (Yao et al., 2016), Dielectric (Zhu et al., 2015), molecular distillation (Berti et al., 2018), label-free proteomics (Han et al., 2022), HPLC-UV detection (Abdellatif et al., 2020), electromagnetic techniques (Wu et al., 2021), and Nuclear Magnetic Resonance (NMR) (Sacchi et al., 2018). However, limitations such as extended evaluation time, high instrumentation costs, intricate sample pre-treatment, and the demand for specialized expertise in measurements and analysis have been associated with these approaches. Imaging technologies in food science not only enhance the quality and safety aspects but also offer economic benefits through lower costs and increased processing speed. Providing real-time, reliable analysis makes them a valuable tool in modern food industry, contributing to improved efficiency, safety and sustainability (Azimi-Saghin et al., 2023; Hosainpour et al., 2022; Kheiralipour et al., 2022; Kheiralipour & Nargesi, 2024; Nargesi & Kheiralipour, 2024; Salam et al., 2022). Phillips et al. explored the influence of fat on sensory attributes, viscosity, and color of low-fat milk, finding significant effects on color components (L*, a*, b*). Notably, variations in milk fat content led to alterations in surface color, such as increased whiteness and decreased green and blue tones (Phillips et al., 1995).

Recent studies have illuminated the viability of image processing technology for milk quality assessment and quantification (Djaowé et al., 2013; Ramos et al., 2021), as well as the application of artificial neural networks (ANNs) for detecting adulterants in milk (Amsaraj et al., 2021; Sharifi et al., 2023) and analyzing diverse products (Ali et al., 2021; Espejo-Carpio et al., 2018; Kumar et al., 2020; Kumar et al., 2019). Additionally, ANN demonstrated superior predictive accuracy for initial-day milk yield compared to other methodologies (Dallago et al., 2019). The particle swarm optimization (PSO), known for numerical optimization tasks (Gui et al., 2022), has gained prominence for solving a range of problems across science and engineering (Chaudhary et al., 2020; Rajeshkumar et al., 2023).

Monitoring the milk fat content of cows not only yields critical information about farm health but also facilitates the expedient evaluation of milk quality. However, the investigation remains absent regarding using color features for milk property monitoring, even though clustering and optimization techniques such as PSO can be integrated with image processing. Noteworthy studies have incorporated image analysis to quantify lactobacilli bacteria in milk (Borin et al., 2007), predicted milk fat content using optical techniques (Ragni et al., 2016), assessed milk with optical spectrometry (Rozycki et al., 2010), and evaluated milk color using colorimetric vision machines (Milovanovic et al., 2021).

Ming et al. applied ANN combined with PSO for modeling coconut milk spray drying, highlighting the method's enhanced predictive accuracy. Building on these insights, our study aims to employ image processing, ANN, and PSO to swiftly and reliably monitor milk fat content. Our objectives encompass (i) characterizing milk color through digital imagery and MATLAB-based image processing, (ii) tracking color shifts in milk with varying fat content, (iii) utilizing PSO to optimize coefficients for input parameters in ANN, and (iv) leveraging the optimized image-derived features to differentiate between distinct milk fat levels using the developed ANN model (Ming et al., 2021).

MATERIALS AND METHODS

Sample preparation

A total number of 150 samples of pure milk, each containing 100ml, were meticulously prepared at a research institute dedicated to dairy cattle farming in Karaj, Iran. The initial step involved obtaining ten reference samples, which were skimmed to create a benchmark. Subsequently, 14 distinct fat levels were introduced to the remaining samples, with each group comprising ten samples to achieve the desired fat content (Table 1).

Table 1. Amount of classified milk fat content and replications to determine a relation among the color features and milk fat (Amount of fat content was made by adding specified amount of cream with 50 % fat to the first 0.2 % fat content)

Group	1 (reference)	2	3	4	5	6	7	8	9	10	11	12	13	14	15
Milk fat (%)	0	0.2	0.5	0.8	1.0	1.3	1.5	1.7	1.8	2.2	2.4	2.9	3.0	3.2	3.5
Replication	10	10	10	10	10	10	10	10	10	10	10	10	10	10	10

The presence of fat in milk was observed as minute globules characterized by a size range specific to each individual sample, enveloped by membrane proteins. All samples were subjected to homogenization using an ELMA ultrasonic homogenizer to ensure uniformity. While this process sacrificed color texture information, rendering the samples unsuitable for extended longitudinal studies, it proved effective for quality control when dealing with samples featuring diverse and consistent surfaces. The evaluation of ultrasonic homogenizer performance entailed considering factors such as apparatus frequency, setting time for samples in the equipment, and the probe diameter, in accordance with the methodology outlined in Correa et al. (Correa et al., 2022). Additionally, Ertugay et al. reported that employing a vibration amplitude of 40% for 10 minutes in milk homogenization yielded results comparable to those achieved through industrial homogenization. Hence, using the ultrasonic homogenizer, a probe diameter of 10 mm, a setting time of 10 minutes, and an optimized vibration amplitude were chosen for the homogenization process (Ertugay et al., 2004).

Following the homogenization step, the milk samples were used to establish a correlation between color attributes and milk fat content.

Image acquisition and capture

The milk samples, enclosed within Petri plates, were positioned within a lightbox measuring 45×45×40 cm^3. The ensuing images were captured, as depicted in Figure 1. The orientation of the samples within the light box was randomized. A digital color camera (Model G7, Canon, Japan) was employed for image recording, boasting a resolution of 480 × 640 pixels. The camera was situated vertically above the lightbox, initially positioned at a distance of 30 cm—adjustable along a fixed rail.

Figure 1. Schematic representation of light box with adjustable light using different light sources and changeable camera distance

To ensure effective background subtraction via standard segmentation routines, a black textile was employed as the backdrop. This choice was driven by the pronounced color contrast between the samples and the background (Demir et al., 2018). Several lighting options were evaluated against six crucial parameters, detailed in Table 2, to identify a dependable light source (Hornberg, 2017). The performance rating is based on a scale of 1 to 5, with 5 denoting the highest performance and 1 indicating the lowest for each parameter.

Table 2. Comparison of different lamps to select an available light source

Index	Halogen	Xenon	Laser	LED	Fluorescent
Life time	1	4	3	5	5
Heat generation	1	3	3	5	5
Reaction time	1	5	1	5	5
Intensity	5	5	3	4	4
Aging and drift	1	2	3	5	5
Cost	3	3	4	4	2
Total	12	22	17	28	26

Subsequently, LED and fluorescent lamps were selected as the illumination sources due to their superior performance and larger dimensions compared to xenon, halogen, and laser alternatives. The lighting configuration employed a combination of a circular fluorescent lamp (32 cm external diameter, 32 W, T9) centrally positioned within the lightbox and four LED lamps (3 W) arranged at the corners of a square measuring 32 cm on each side. The collective output of these sources focused at the center of the box, generating an optimal illumination setup.

Image segmentation and filtration

The image analysis process employed the image segmentation technique, which involves dividing an image into distinct sections or objects. Central to this approach is thresholding—an essential step in image segmentation—where a constant value is applied under consistent environmental conditions. For this research, the threshold was computed using a mask derived from the covariance matrix of a designated segment within each sample.

Flickering is a challenge when utilizing fluorescent lamps (Ghosh et al., 2018). Addressing this issue is pivotal to ensure uniform illumination across all images. To achieve this objective, linear filtering was implemented, including edge sharpening, noise reduction, equalization of illumination, and even deconvolution to counteract blur and motion effects. These tasks involve convolving the original image with a suitable filter kernel to generate the filtered image. A significant hurdle in image convolution lies in the substantial computational demands, often leading to impractical execution times. To mitigate this, convolution by separation and FFT (Fast Fourier Transform) convolution were employed, effectively reducing execution times (Gholami & Farshad, 2019).

From the filtered and segmented images, a set of parameters corresponding to color attributes were extracted and determined.

Color analysis

The color images, initially represented in the RGB system, wherein each pixel comprises three color components—red (R), green (G), and blue (B)—underwent a series of transformations. They were first converted into the HSI color space and subsequently into the CIE Lab color space using a nonlinear transformation method akin to that employed by Asmare et al. (Asmare et al., 2015). This transition was necessary for developing image processing algorithms founded upon color descriptions that resonate naturally and intuitively with human perception.

In the HSI color space, H (hue) characterizes pure colors, such as pure yellow, orange, or red. The parameter S (saturation) quantifies the degree to which a pure color is diluted by white light, while I (brightness) is a subjective attribute that remains challenging to measure quantitatively. Parameter I encapsulate the achromatic concept of intensity and play a pivotal role in expressing color sensation (Cereceda et al., 2022). The RGB-to-HSI conversion was carried out using Equations (1–3) as follows:

$$I = \frac{1}{3}(R+G+B) \tag{1}$$

$$S = 1 - \frac{3}{(R+G+B)}[\min(R,G,B)] \tag{2}$$

$$\theta = \arccos\{\frac{[(R-G)+(R-B)]/2}{[(R-G)^2+(R-B)(G-B)]^{1/2}}\}$$
$$H = \begin{cases}\theta & B \le G \\ 360-\theta & B > G\end{cases} \tag{3}$$

Normalized H values spanned a range of 0 to 1 after being divided by 360°. The remaining two HSI components naturally resided in this interval, provided that the given RGB values fall within the [0, l] range.

The CIE Lab (L*a*b*) color space was valued for its colorimetric, perceptually uniform, and device-independent attributes. The L* component signifies luminance or lightness, ranging from 0 (black) to 100 (white). Meanwhile, the chromatic components a* and b* span from green to red and blue to yellow, respectively, with values encompassing the range of -120 to 120.

The milk surface images underwent analysis via MATLAB 7.12 implementation. Mean values of R, G, B, H, S, I, L*, a*, and b* across different color spaces were extracted and reported.

Furthermore, several color features were computed for each color component using Equations (4–7):

Mean: Representing the average intensity of each component as:

$$x = \frac{1}{N}\sum_{i=1}^{N} x_i \tag{4}$$

Standard deviation: Indicating the average contrast as:

$$\sigma = \sqrt{\frac{1}{N}\sum_{i=1}^{N}(x_i-\mu)^2} \tag{5}$$

Kurtosis: Measuring the peaked Ness of a local histogram as:

$$k = E(\frac{x-\mu}{\sigma})^4 \tag{6}$$

Skewness: Quantifying the deviation of the local histogram from symmetry as:

$$\gamma = E(\frac{x-\mu}{\sigma})^3 \quad (7)$$

Variance: Expressing the degree of variation around the averages.

Entropy: Reflecting the level of randomness.

Energy: Signifying energy in 2-D wavelet decomposition.

These calculations and transformations were fundamental to extracting meaningful features from the color spaces and contributing to subsequent analysis (Attallah et al., 2019).

Particle swarm optimization method (PSO)

To deduce the optimization coefficients and subsequently adjust them to the color features, effectively preparing them for utilization as input parameters for ANN, the particle swarm optimization (PSO) algorithm was implemented.

The updating of the velocity (v_i) and position (x_i) for the i^{th} particle adheres to the following equations:

$$v_i(t+1) = w \times v_i(t) + c1 \times rand1 \times (pbest_i - x_i(t)) + c2 \times rand1 \times (gbest - x_i(t)) \quad (8)$$

$$x_i(t+1) = x_i(t) + v_i(t+1) \quad (9)$$

In these equations, pbest signifies the best previous position resulting in the optimal fitness value for the i^{th} particle, while gbest denotes the best position identified across the entire population. Constants c1 and c2 are acceleration factors set to 2 in this study. Meanwhile, w denotes the inertia weight, representing the weighing of stochastic acceleration terms that influence each particle's movement towards both the pbest and gbest positions. The value of w was computed for each iteration (Shi & Eberhart, 2001). Random numbers rand1 and rand2, spanning the range (0,1), contribute to the stochastic nature of the PSO algorithm.

Upon concluding iterations, a significant portion of particles is anticipated to converge within a narrow vicinity around the global optima within the search space. The canonical PSO has been subject to empirical and theoretical examinations by numerous researchers (Shi & Eberhart, 2001). However, it is worth noting that premature convergence can occur if the swarm employs a diminutive inertia weight (w) or constriction coefficient in various scenarios.

Artificial neural network (ANN)

In this study, the estimation of milk fat content was executed through the utilization of an Artificial Neural Network (ANN), employing the Multi-layer Perceptron (MLP) architecture along with the backpropagation (BP) algorithm. The network structure comprised an input layer, three hidden layers, and an output layer, as depicted in Figure 2.

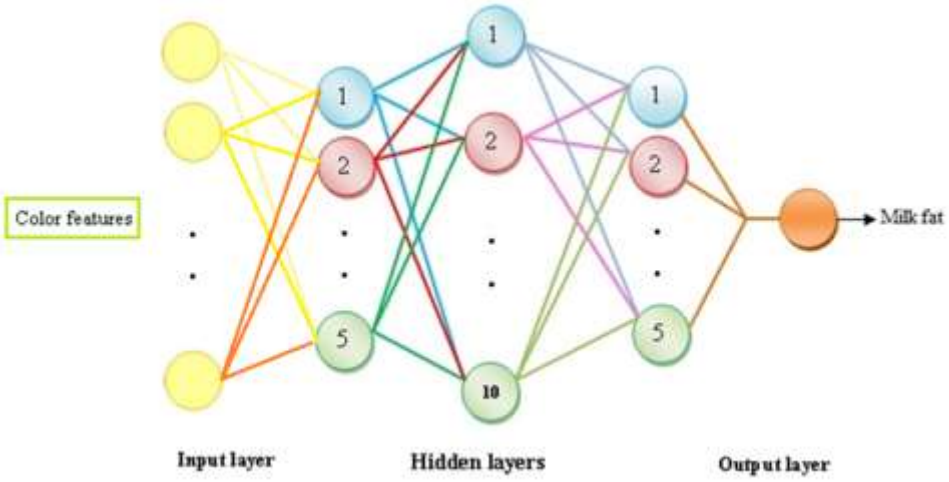

Fig ure2. Neural network architecture

The input layer featured 63 nodes, corresponding to the 21 features in each color space. The number of nodes in the output layer matched the quantity of distinct milk fat classes. The selection of nodes for the hidden layers was guided by empirical assessment to optimize system performance. To ascertain an optimal configuration, the training commenced with a subset of datasets, given the limitations of available milk samples. This training process was iteratively performed until the final number of hidden nodes was achieved, often following a pattern such as 5-10-5.

The employed ANN incorporated a nonlinear hyperbolic tangent activation function. The training was guided by a set of training goal, a learning rate, and a momentum term set at 0.003, 0.9, and 0.9, respectively. To expedite and enhance training accuracy, the network inputs were scaled by the optimization coefficients derived from the PSO method.

A distinctive aspect of this study, up until the present date, lies in the application of image processing technology combined with PSO and ANN methodologies to monitor milk fat content. This innovative approach offers rapidity, cost-efficiency, and reliability, presenting a novel solution that has not been previously explored in milk fat assessment.

RESULTS AND DISCUSSIONS

Color features

The normalized mean color components of milk fat groups, based on their color components using LED, fluorescent, and a combination of LED and fluorescent sources, are illustrated in Figure 3.

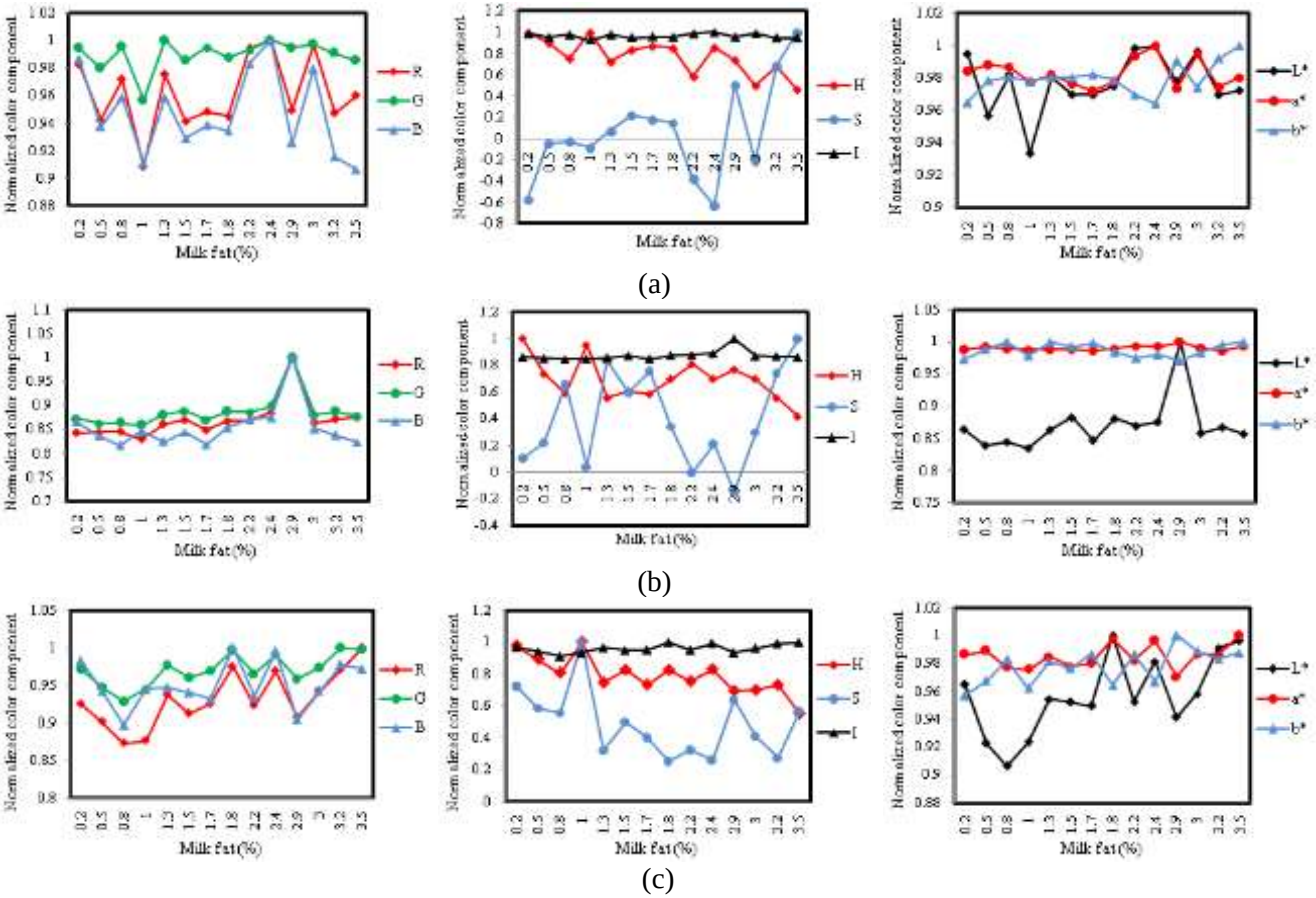

Figure 3. Normalized form of mean color components with different illuminations; (a) Fluorescent; (b) LED; (c) Combination of LED and fluorescent

When evaluating the RGB factors for three types of light sources—LED, fluorescent, and the combined LED-florescent—it is evident that the distribution of G (green) has a narrower spread in comparison to R (red) and B (blue). This suggests that variations in milk color are predominantly influenced by red and blue colors, as opposed to green. A similar phenomenon has been observed in studies exploring the progressive lighting of a tungsten lamp and its effect on milk color (Ragni et al., 2016). Notably, the distribution of RGB factors under fluorescent lighting is the most constrained, rendering it unsuitable for assessing milk fat content based on RGB factors. However, the RGB distribution under the combined LED-florescent lighting exhibits a broader range (0.86 – 1) than the LED light range (0.91 – 1).

In terms of H (hue), S (saturation), and I (brightness) factors, I component displays the narrowest range, while S exhibits the broadest range across all light sources. The range of the S factor varies from (-0.6 – 1) to (-0.2 – 1) and (0.2 – 1) for LED, fluorescent, and LED-florescent lighting, respectively.

Regarding L*, a*, and b* components, the combined LED fluorescent lighting demonstrates a more dispersed allocation than other light sources. This suggests that the RGB and L*a*b* factors are more promising as segregation criteria. Moreover, the combination of LED and fluorescent illumination yields the most favorable results among the tested lighting conditions.

Considering other color features, such as standard deviation, kurtosis, skewness, variance, entropy, and energy, there were no discernible differences in the milk fat content assessment using different illumination methods. Consequently, the combined LED-florescent light emerges as the superior performer in RGB and L*a*b* factors, while fluorescent light performs better with H, I, and S components.

Further studies determined that for homogenization purposes of milk surfaces, images were recorded and subsequently cropped into four different sizes: 50×50, 100×100, 200×200, and 400×400 pixels. As indicated in Figure 4, color components determined from these cropped images exhibited minimal variations across the different sizes. Notably, B (blue) and L* (luminance/lightness) components displayed the most minor variability among all the color components when considering different image sizes.

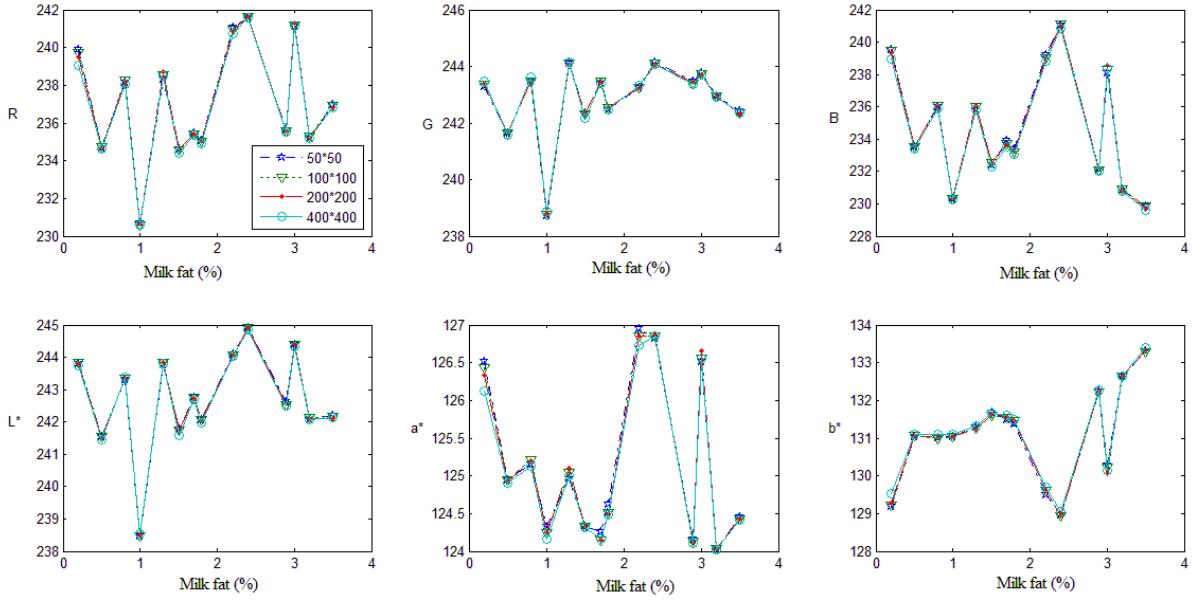

Figure 4. Color components determined from picture with different cropped sizes

PSO Optimization

The primary objective of employing the PSO method was to enhance the monotonous behavior of color features. The optimized color features attained through LED, fluorescent, and their combined illumination are visualized in Figure 5.

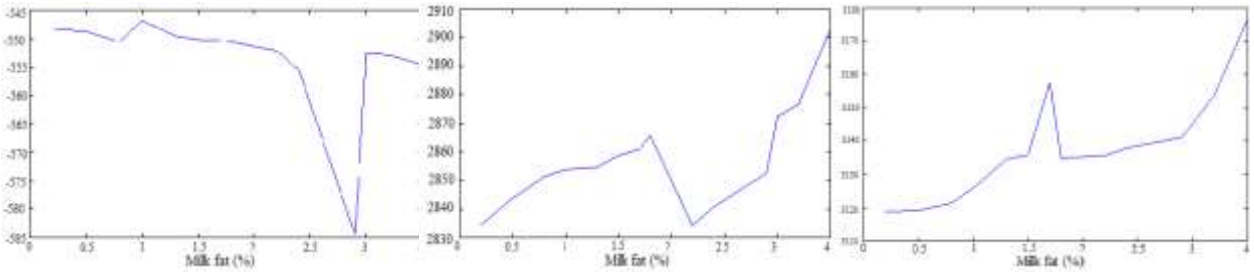

(a) (b) (c)

Figure 5. Optimized color features using different illumination; (a) LED illumination; (b) Florescent illumination; (c) Combination of LED and florescent

Observations reveal that under LED illumination (a), the optimization features exhibit an error in fat content ranging between 2.9–3.1%, with a disorderly descending pattern. On the other hand, fluorescent illumination (b) yields an error in fat content ranging from 1.7–2.2%, displaying a disorderly ascending pattern. Notably, the combination of LED and fluorescent illumination (c) showcases shorter disorderly monotonicity in the optimization features. This combination illumination approach aligns well with the determined color features, making it the superior input dataset for the developed Artificial Neural Network (ANN).

This comparison underscores the combined LED-florescent illumination's effectiveness in enhancing the monotonous nature of color features, ultimately contributing to more accurate milk fat content estimation.

Artificial neural network (ANN)

In this study, the ANN was considered for different illuminations. Because of the lack of milk fat samples for training data, the first 13 datasets were explicitly used as training, and the rest of the dataset were used as testing for both LED and florescent illuminations. The accuracy of the network is presented in Table 3 using statistical parameters. Furthermore, the final estimated milk fat using ANN, along with their errors, is given in Table 4.

Table 3. Accuracy of designed artificial neural network (ANN) for different illumination

Illumination	MSE	MAE	R^2
LED	0.20	0.40	0.84
Florescent	0.19	0.34	0.78
Combination	0.05	0.22	0.99

Table 4. Estimated amount of milk fat using artificial neural network (ANN)

Illumination	Real amount	Estimated amount	Absolute error	Relative error
LED	3.2	3.5	0.3	0.094
	1.8	1.9	0.1	0.056
	1.3	0.7	0.6	0.460
	2.9	2.5	0.4	0.140
	0.2	0.8	0.6	3.000
Florescent	2.2	1.7	0.5	0.230
	2.4	2.2	0.2	0.083
	1.0	1.2	0.2	0.200
	1.7	1.7	0	0.000
	0.5	1.3	0.7	1.400
Combination	2.9	2.7	0.2	0.069
	0.2	0.5	0.3	1.500
	2.2	2.0	0.2	0.091
	1.3	1.5	0.2	0.150
	3.5	3.3	0.2	0.057

The least mean square error (MSE=0.05), mean absolute error (MAE=0.22), and the most root square (R^2=0.99) represent higher efficiency of the combination of florescent and LED than their separated illuminations. Similar prediction results have been obtained with R^2 up to 0.997 by using ANN for the prediction of the fat content of commercialized milk (Ragni et al., 2016).

Effect of water on color components

To explore the influence of water on the constituent properties of milk, both low-fat (1.5%) and high-fat (3%) milk were investigated in conjunction with varying percentages of water content (25%, 50%, and 75%). The RGB color components were assessed, as shown in Figure 6.

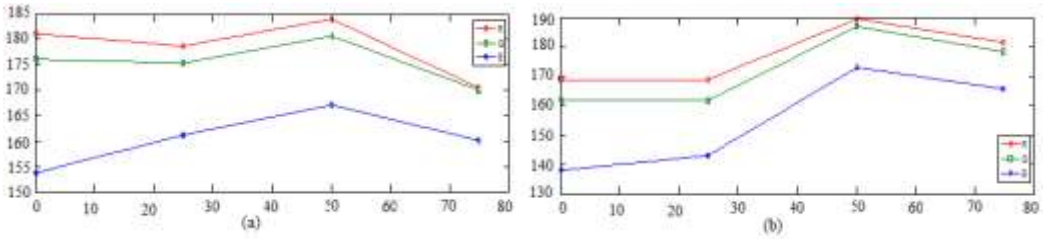

Figure 6. Effect of milk water on its RGB color components; (a) 1.5 % milk fat; (b) 3 % milk fat

The results reveal that when the water content in milk is increased by 50%, a notable increase is discerned. This increase is more pronounced in milk with a fat content of 3% compared to that with 1.5% fat. However, it is essential to acknowledge that the inherent variability in outdoor lighting conditions could constrain the application of these findings in real-life scenarios.

Through the analysis, it became evident that a dataset of image color features utilizing a reduced set of R, B, S, H, and L* features exhibited the most favorable results for estimating milk fat content in this study. Importantly, this selection eliminated intensity features that might be less

beneficial in highly variable outdoor lighting conditions. These findings correlate with earlier research that indicated a strong and non-linear relationship with fat content (R^2 up to 0.985) using voltage waveform methodology [11]. In another study, high correlations (0.934 <= r <= 0.990; alpha = 0.006 - 0.000) between raw milk fat content and parallel equivalent capacitance values were reported (Żywica et al., 2012).

Furthermore, the study confirmed that these methodologies can effectively monitor milk fat content under controlled laboratory lighting conditions. The determination of color components exhibited significant disparities across different percentages of mixed milk-water compositions. These results prove that color feature-based estimation holds promise for monitoring milk fat content. Consequently, combining ANN-based image processing with the PSO technique is a rapid, reliable, and cost-effective means for monitoring milk fat content. This approach holds particular value for dairy cattle farming and the development of devices for online monitoring of milk fat content.

CONCLUSION

This paper introduces a pioneering approach, combining an optimized Artificial Neural Network (ANN) with image processing using the particle swarm optimization (PSO) technique to cluster complex data effectively. A salient feature of this method is its ability to assess comprehensive variations in milk fat content quantitatively. The outcomes showcased the superior efficacy of employing a combined LED and fluorescent light source over their implementations, yielding minimal mean square error (MSE=0.05), mean absolute error (MAE=0.22), and a high coefficient of determination (R2=0.99). The integration of ANN with the optimized dataset obtained through PSO exhibited an enhanced performance, underscoring the potential of this proposed method to bolster the precision of milk fat content estimation. Additionally, the approach establishes a solid technical foundation for real-time quality milk monitoring. By employing image processing, the technique adeptly captures spatial changes and effectively measures and analyzes color transformations that correspond to milk fat variations, thus facilitating content monitoring via ANN.

Notably, the proposed technique boasts simplicity, versatility, and a cost-effective nature, rendering it an accessible method with applicability across a broad spectrum of scenarios. In summary, this paper presents a significant advancement in the realm of milk fat content estimation and quality monitoring, leveraging innovative methods to achieve accurate and efficient results.

Data Availability Statement

The datasets generated and/or analyzed during the current study are available from the corresponding author on reasonable request.

Compliance with Ethical Standards:

Funding

This work was supported by University of Tehran, College of Agriculture Natural Resources, Grant Number 120041.

Conflict of interest

The authors declare that they have no conflict of interest.

Ethical approval

This paper does not contain any studies with human participants or animals performed by any of the authors.

REFERENCES

Abdellatif, A. A., El Hamd, M. A., Salman, K. H., Abd-El-Rahim, A. M., El-Maghrabey, M., & Tawfeek, H. M. (2020). Integrative physicochemical and HPLC assessment studies for the inclusion of lornoxicam in buffalo's milk fat globules as a potential carrier delivery system for lipophilic drugs. *Microchemical Journal*, *152*, 104321. https://doi.org/10.1016/j.microc.2019.104321

Ali, A. H., Wei, W., Khalifa, S. A., Zhang, X., & Wang, X. (2021). Effect of pasteurisation, homogenisation and freeze-drying on bovine and buffalo milk fat triacylglycerols profile. *International Journal of Dairy Technology*, *74*(3), 472-488. https://doi.org/10.1111/1471-0307.12781

Ali, F. (2022). Nonthermal and thermal treatments impact the structure and microstructure of milk fat globule membrane. *International Journal of Dairy Technology*, *75*(2), 338-347. https://doi.org/10.1111/1471-0307.12840

Amsaraj, R., Ambade, N. D., & Mutturi, S. (2021). Variable selection coupled to PLS2, ANN and SVM for simultaneous detection of multiple adulterants in milk using spectral data. *International Dairy Journal*, *123*, 105172. https://doi.org/10.1016/j.idairyj.2021.105172

Asmare, M. H., Asirvadam, V. S., & Hani, A. F. M. (2015). Image enhancement based on contourlet transform. *Signal, Image and Video Processing*, *9*, 1679-1690. https://doi.org/10.1007/s11760-014-0626-7

Attallah, B., Serir, A., & Chahir, Y. (2019). Feature extraction in palmprint recognition using spiral of moment skewness and kurtosis algorithm. *Pattern Analysis and Applications*, *22*, 1197-1205. https://doi.org/10.1007/s10044-018-0712-5

Azimi-Saghin, B., Omid, M., Rezvani, F., & Arefi, M. (2023). An Algorithm to Extract the Defective Areas of Potato Tubers Infected with Black Scab Disease Using Fuzzy C Means Clustering for Automatic Grading. *Biomechanism and Bioenergy Research*, *2*(1), 32-39. https://doi.org/10.22103/bbr.2023.21783.1046

Berti, J., Grosso, N. R., Fernandez, H., Pramparo, M. C., & Gayol, M. F. (2018). Sensory quality of milk fat with low cholesterol content fractioned by molecular distillation. *Journal of the Science of Food and Agriculture*, *98*(9), 3478-3484. https://doi.org/10.1002/jsfa.8866

Borin, A., Ferrão, M. F., Mello, C., Cordi, L., Pataca, L. C., Durán, N., & Poppi, R. J. (2007). Quantification of Lactobacillus in fermented milk by multivariate image analysis with least-squares support-vector machines. *Analytical and bioanalytical chemistry*, *387*, 1105-1112. https://doi.org/10.1007/s00216-006-0971-7

Cereceda, D., Medel-Vera, C., Ortiz, M., & Tramon, J. (2022). Roughness and condition prediction models for airfield pavements using digital image processing. *Automation in Construction*, *139*, 104325. https://doi.org/10.1016/j.autcon.2022.104325

Chaudhary, A., Thakur, R., Kolhe, S., & Kamal, R. (2020). A particle swarm optimization based ensemble for vegetable crop disease recognition. *Computers and Electronics in Agriculture*, *178*, 105747. https://doi.org/10.1016/j.compag.2020.105747

Correa, K. d. P., Silva, M. E. T. d., Oliveira, D. R. B. d., Oliveira, A. F. d., Santos, I. J. B., Oliveira, E. B. d., & Coimbra, J. S. d. R. (2022). Influence of homogenization in the physicochemical quality of human milk and fat retention in gastric tubes. *Journal of Human Lactation*, *38*(2), 309-322. https://doi.org/10.1177/08903344211031456

Dallago, G. M., de Figueiredo, D. M., de Resende Andrade, P. C., dos Santos, R. A., Lacroix, R., Santschi, D. E., & Lefebvre, D. M. (2019). Predicting first test day milk yield of dairy heifers. *Computers and Electronics in Agriculture*, *166*, 105032. https://doi.org/10.1016/j.compag.2019.105032

Demir, B., Sayıncı, B., Çetin, N., Yaman, M., Çömlek, R., Aydın, Y., & Sutyemez, M. (2018). Elliptic Fourier based analysis and multivariate approaches for size and shape distinctions of walnut (Juglans regia L.) cultivars. *Grasas y Aceites*, *69*(4), e271-e271. https://doi.org/10.3989/gya.0104181

Djaowé, G., Bitjoka, L., Boukar, O., Libouga, D. G., & Waldogo, B. (2013). Measurement of the rennet clotting time of milk by digital image sequences (2D+ t) processing. *Journal of Food Engineering*, *114*(2), 235-241. https://doi.org/10.1016/j.jfoodeng.2012.07.024

Eid, S. M., El-Shamy, S., & Farag, M. A. (2022). Identification of milk quality and adulteration by surface-enhanced infrared absorption spectroscopy coupled to artificial neural networks using citrate-capped silver nanoislands. *Microchimica Acta*, *189*(8), 301. https://doi.org/10.1007/s00604-022-05393-4

Ertugay, M. F., ŞENGÜL, M., & ŞENGÜL, M. (2004). Effect of ultrasound treatment on milk homogenisation and particle size distribution of fat. *Turkish Journal of Veterinary & Animal Sciences*, *28*(2), 303-308.

Espejo-Carpio, F. J., Pérez-Gálvez, R., Guadix, A., & Guadix, E. M. (2018). Artificial neuronal networks (ANN) to model the hydrolysis of goat milk protein by subtilisin and trypsin. *Journal of Dairy Research*, *85*(3), 339-346. https://doi.org/10.1017/S002202991800064X

Gallier, S., Gragson, D., Jiménez-Flores, R., & Everett, D. W. (2010). Surface characterization of bovine milk phospholipid monolayers by Langmuir isotherms and microscopic techniques. *Journal of agricultural and*

food chemistry, *58*(23), 12275-12285. https://doi.org/10.1021/jf102185a

Gholami, A., & Farshad, M. (2019). Fast hyperbolic Radon transform using chirp-z transform. *Digital Signal Processing*, *87*, 34-42. https://doi.org/10.1016/j.dsp.2019.01.003

Ghosh, A., Seth, S. K., & Purkayastha, P. (2018). Undulation induced tuning of electron acceptance by edge-oxidized graphene oxide. *Spectrochimica Acta Part A: Molecular and Biomolecular Spectroscopy*, *204*, 425-431. https://doi.org/10.1016/j.saa.2018.06.052

Gui, H., Xiang, J., Xing, T., Liu, J., Chu, Z., He, X., & Liu, C. (2022). Boundary element method with particle swarm optimization for solving potential problems. *Advances in Engineering Software*, *172*, 103191. https://doi.org/10.1016/j.advengsoft.2022.103191

Han, B., Zhang, L., & Zhou, P. (2022). Comparison of milk fat globule membrane protein profile among bovine, goat and camel milk based on label free proteomic techniques. *Food Research International*, *162*, 112097. https://doi.org/10.1016/j.foodres.2022.112097

Hornberg, A. (2017). *Handbook of machine and computer vision: the guide for developers and users*. John Wiley & Sons.

Hosainpour, A., Kheiralipour, K., Nadimi, M., & Paliwal, J. (2022). Quality assessment of dried white mulberry (Morus alba L.) using machine vision. *Horticulturae*, *8*(11), 1011. https://doi.org/10.3390/horticulturae8111011

Kheiralipour, K., Nadimi, M., & Paliwal, J. (2022). Development of an intelligent imaging system for ripeness determination of wild pistachios. *Sensors*, *22*(19), 7134. https://doi.org/10.3390/s22197134

Kheiralipour, K., & Nargesi, M. H. (2024). Classification of wheat flour levels in powdered spices using visual imaging. *Journal of Agriculture and Food Research*, *18*, 101408. https://doi.org/10.1016/j.jafr.2024.101408

Kumar, R., Rao, P. S., Rana, S. S., & Ghosh, P. (2020). Comparative performance analysis of enzyme inactivation of soy milk by using RSM and ANN. *Journal of Food Process Engineering*, *43*(11), e13530. https://doi.org/10.1111/jfpe.13530

Kumar, V., Chakravarty, A., Magotra, A., Patil, C., & Shivahre, P. (2019). Comparative study of ANN and conventional methods in forecasting first lactation milk yield in Murrah buffalo. *Indian Journal of Animal Sciences*, *89*(11), 1262-1268. https://doi.org/10.56093/ijans.v89i11.95887

Li, S., Yang, Y., Chen, C., Li, L., Valencak, T. G., & Ren, D. (2021). Differences in milk fat globule membrane proteins among Murrah, Nili-Ravi and Mediterranean buffaloes revealed by a TMT proteomic approach. *Food Research International*, *139*, 109847. https://doi.org/10.1016/j.foodres.2020.109847

McCarthy, K., Lopetcharat, K., & Drake, M. (2017). Milk fat threshold determination and the effect of milk fat content on consumer preference for fluid milk. *Journal of Dairy Science*, *100*(3), 1702-1711. https://doi.org/10.3168/jds.2016-11417

Milovanovic, B., Tomovic, V., Djekic, I., Miocinovic, J., Solowiej, B. G., Lorenzo, J. M., . . . Tomasevic, I. (2021). Colour assessment of milk and milk products using computer vision system and colorimeter. *International Dairy Journal*, *120*, 105084. https://doi.org/10.1016/j.idairyj.2021.105084

Ming, J. L. K., Anuar, M. S., How, M. S., Noor, S. B. M., Abdullah, Z., & Taip, F. S. (2021). Development of an artificial neural network utilizing particle swarm optimization for modeling the spray drying of coconut milk. *Foods*, *10*(11), 2708. https://doi.org/10.3390/foods10112708

Moate, P., Jacobs, J., Hannah, M., Morris, G., Beauchemin, K., Hess, P. A., . . . Wales, W. (2018). Adaptation responses in milk fat yield and methane emissions of dairy cows when wheat was included in their diet for 16 weeks. *Journal of Dairy Science*, *101*(8), 7117-7132. https://doi.org/10.3168/jds.2017-14334

Mu, S., Stieger, M., & Boesveldt, S. (2022). Olfactory discrimination of fat content in milks is facilitated by differences in volatile compound composition rather than odor intensity. *Food Chemistry*, *393*, 133357. https://doi.org/10.1016/j.foodchem.2022.133357

Nargesi, M. H., & Kheiralipour, K. (2024). Ability of visible imaging and machine learning in detection of chickpea flour adulterant in original cinnamon and pepper powders. *Heliyon*, *10*(16). https://doi.org/10.1016/j.heliyon.2024.e35944

Phillips, L. G., Mcgiff, M. L., Barbano, D. M., & Lawless, H. T. (1995). The influence of fat on the sensory properties, viscosity, and color of lowfat milk. *Journal of Dairy Science*, *78*(6), 1258-1266. https://doi.org/10.3168/jds.S0022-0302(95)76746-7

Pluschke, A., Gilbert, M., Williams, B., van den Borne, J., Schols, H., & Gerrits, W. (2016). The effect of replacing lactose by starch on protein and fat digestion in milk-fed veal calves. *animal*, *10*(8), 1296-1302. https://doi.org/10.1017/S1751731116000252

Ragni, L., Iaccheri, E., Cevoli, C., & Berardinelli, A. (2016). Spectral-sensitive pulsed photometry to predict the fat content of commercialized milk. *Journal of Food Engineering*, *171*, 95-101. https://doi.org/10.1016/j.jfoodeng.2015.10.017

Rajeshkumar, G., Kumar, M. V., Kumar, K. S., Bhatia, S., Mashat, A., & Dadheech, P. (2023). An Improved Multi-Objective Particle Swarm Optimization Routing on MANET. *Computer Systems Science & Engineering*, *44*(2), 1187-1200. https://doi.org/10.32604/csse.2023.026137

Ramos, A. S., Fontes, C. H., Ferreira, A. M., Baccili, C. C., da Silva, K. N., Gomes, V., & de Melo, G. J. A. (2021). Somatic cell count in buffalo milk using fuzzy clustering and image processing techniques. *Journal of Dairy Research*, *88*(1), 69-72. https://doi.org/10.1017/S0022029921000042

Rozycki, S. D., Buera, M. d. P., Piagentini, A., Costa, S. C., & Pauletti, M. (2010). Advances in the study of the kinetics of color and fluorescence development in concentrated milk systems. *Journal of Food Engineering*, *101*(1), 59-66. https://doi.org/10.1016/j.jfoodeng.2010.06.009

Sacchi, R., Paduano, A., Caporaso, N., Picariello, G., Romano, R., & Addeo, F. (2018). Assessment of milk fat content in fat blends by 13C NMR spectroscopy analysis of butyrate. *Food Control*, *91*, 231-236. https://doi.org/10.1016/j.foodcont.2018.04.011

Salam, S., Kheiralipour, K., & Jian, F. (2022). Detection of unripe kernels and foreign materials in chickpea mixtures using image processing. *Agriculture*, *12*(7), 995. https://doi.org/10.3390/agriculture 12070995

Sharifi, F., Naderi-Boldaji, M., Ghasemi-Varnamkhasti, M., Kheiralipour, K., Ghasemi, M., & Maleki, A. (2023). Feasibility study of detecting some milk adulterations using a LED-based Vis-SWNIR photoacoustic spectroscopy system. *Food Chemistry*, *424*, 136411. https://doi.org/10.1016/j.foodchem.2023.136411

Shi, Y., & Eberhart, R. C. (2001). Fuzzy adaptive particle swarm optimization. Proceedings of the 2001 congress on evolutionary computation (IEEE Cat. No. 01TH8546),

Soukoulis, C., Lyroni, E., & Tzia, C. (2010). Sensory profiling and hedonic judgement of probiotic ice cream as a function of hydrocolloids, yogurt and milk fat content. *LWT-Food Science and Technology*, *43*(9), 1351-1358. https://doi.org/10.1016/j.lwt.2010.05.006

Wu, S., Zhang, H., Jin, Y., Yang, N., Xu, X., & Xie, Z. (2021). Assessment of milk fat based on signal-to-ground voltage. *Journal of Food Measurement and Characterization*, *15*, 1385-1394. https://doi.org/10.1007/s11694-020-00733-5

Xu, W., Bai, J., Peng, J., Samanta, A., & Chang, Y.-T. (2014). Milk quality control: instant and quantitative milk fat determination with a BODIPY sensor-based fluorescence detector. *Chemical Communications*, *50*(72), 10398-10401. https://doi.org/10.1039/x0xx00000x

Yao, Y., Zhao, G., Yan, Y., Mu, H., Jin, Q., Zou, X., & Wang, X. (2016). Milk fat globules by confocal Raman microscopy: Differences in human, bovine and caprine milk. *Food Research International*, *80*, 61-69. https://doi.org/10.1016/j.foodres.2015.12.017

Zhu, X., Guo, W., & Liang, Z. (2015). Determination of the fat content in cow's milk based on dielectric properties. *Food and Bioprocess Technology*, *8*, 1485-1494. https://doi.org/10.1007/s11947-015-1508-x

Żywica, R., Banach, J. K., & Kiełczewska, K. (2012). An attempt of applying the electrical properties for the evaluation of milk fat content of raw milk. *Journal of Food Engineering*, *111*(2), 420-424. https://doi.org/10.1016/j.jfoodeng.2012.01.025